Advanced Synthesis & Catalysis

Accepted Article

Title: Activated Hoveyda-Grubbs Olefin Metathesis Catalysts Derived from a Large Scale Produced Pharmaceutical Intermediate—Sildenafil Aldehyde

Authors: Louis Monsigny, Jakub Piątkowski, Damian Trzybiński, Krzysztof Wozniak, Tomasz Nienałtowski, Anna Kajetanowicz, and Karol Grela

To be cited as: *Adv. Synth. Catal.* 10.1002/adsc.202100669

Link to VoR: https://doi.org/10.1002/adsc.202100669

RESEARCH ARTICLE

DOI: 10.1002/adsc.202100669

Activated Hoveyda-Grubbs Olefin Metathesis Catalysts Derived from a Large Scale Produced Pharmaceutical Intermediate—Sildenafil Aldehyde

Louis Monsigny,[a] Jakub Piątkowski,[a] Damian Trzybiński,[a] Krzysztof Woźniak,[a] Tomasz Nienałtowski,[a,b] Anna Kajetanowicz,[a,*] and Karol Grela[a,*]

[a] Biological and Chemical Research Centre, Faculty of Chemistry, University of Warsaw, Żwirki i Wigury Street 101, 02-089 Warsaw, Poland
[Karol Grela: karol.grela@gmail.com, Anna Kajetanowicz: a.kajetanowicz@uw.edu.pl]
[b] Polpharma SA Pharmaceutical Works, Pelplinska 19, 83-200 Starogard Gdanski, Poland

Received: ((will be filled in by the editorial staff))

Supporting information for this article is available on the WWW under http://dx.doi.org/10.1002/adsc.201######.((Please delete if not appropriate))

Abstract. Two EWG-activated Hoveyda-Grubbs-type ruthenium complexes (**Sil-II** and **Sil-II'**) were obtained, characterized, and screened in a set of olefin metathesis reactions. These catalysts were conveniently synthesized from a commercially available pharmaceutical building block—Sildenafil aldehyde—in two steps only. Stability and catalytic activity tests disclosed that the bulkier NHC-ligand bearing catalyst **Sil-II'** is visibly more stable and productive than its smaller NHC-analogue **Sil-II**. Good application profile of catalyst **Sil-II'** was confirmed in a set of diverse metathesis reactions including ring-closing metathesis (RCM) and cross-metathesis (CM) of complex polyfunctional substrates of medicinal chemistry interest, including a challenging macrocyclization of the Pacritinib precursor. Compatibility of the new catalyst with various green solvents was checked and metathesis of Sildenafil and Tadalafil-based substrates was successfully conducted in acetone. The mechanism of **Sil-II'** initiation has been investigated through kinetic experiments unveiling that the decrease of the steric hindrance of the chelating alkoxy moiety (from *i*PrO to EtO) favors the interchange initiation pathway over the typical dissociation pathway for other popular 2nd generation Hoveyda-Grubbs catalysts.

Keywords: Catalysis, Olefin metathesis, Electron withdrawing group (EWG), Ruthenium catalysts, N-heterocyclic carbene ligands (NHC), Mechanism

Introduction

The formation of carbon-carbon bonds is a crucial reaction in organic chemistry.[1] Among numerous methods for the creation of C–C bonds,[2] olefin metathesis appears to be a peculiarly important tool.[3] Significantly, the catalytic olefin metathesis reaction can *directly transform* a set of already existing C-C double bonds (*e.g.* in a diene) into valuable product (*e.g.* a cycloalkene) with high precision and selectivity under mild conditions.[4] Since the development of relatively air stable ruthenium based Grubbs' catalyst $(PCy_3)_2(Cl)_2Ru{=}CHPh$ (**Gru-I**, Figure 1),[5] this methodology became broadly employed in organic chemistry, particularly in target oriented synthesis, preparation of polymers, and industrial transformation of renewable materials.[6] Despite the high tolerance toward organic functions and the plethora of applications reported with this catalyst, a relatively low stability of **Gru-I** in solution and a quite high catalyst loading typically used are the limitations of this system. Successive enhancement of the catalysis activity and stability has been achieved, firstly, with the introduction of N-heterocyclic carbene (NHC) ligands such as SIMes (1,3-bis-(2,4,6-trimethylphenyl)-2-imidazolidinylidene) or SIPr (1,3-bis-(2,6-triisopropylphenyl)-2-imidazolidinylidene) leading to the so called 2nd generation Grubbs-type catalysts $(NHC)(PCy_3)(Cl)_2Ru{=}CHPh$ (**Gru-II**, and **Gru-II'**, Figure 1).[7] Another noteworthy improvement in the field of olefin metathesis catalyst was the development of ruthenium-indenylidene complexes (such as **Ind-I** and **Ind-II**, Figure 1) which are readily obtained from $[RuCl_2(PPh_3)_3]$ and 1,1-diphenylpropargyl alcohol and are resistant to harsh conditions such as high temperature.[8] Next milestone was reached when Hoveyda reported ~~on~~ the first phosphine-free Ru complex bearing a bidentate 2-alkoxybenzylidene ligand [(SIMes)(2-isopropoxy-κ-O-benzylidene)$RuCl_2$] (**Hov-II**, Figure 1).[9] Subsequently, the introduction of electron

10.1002/adsc.202100669

withdrawing group (EWG) in the chelating benzylidene moiety of Hoveyda-Grubbs type complexes led to a further increase of the activity and stability of such obtained catalysts enabling the decrease of the catalyst loading concomitantly with an increase in application scope.[10] In this regard, Grela,[11] Zhan,[12] and Mauduit[13] developed several activated derivatives of **Hov-II**, that were substituted in the chelating benzylidene fragment with electron withdrawing groups such as NO_2 (**Gre**), SO_2NMe_2 (**Zha**), and $NHC(O)CF_3$ (**Mau**; Figure 1). Despite their usually higher activity and some promising applications,[14] the synthesis of such catalysts require more synthetic steps as compared to the parental unsubstituted **Hov-II** complex.[15] Consequently, finding a commercially available building block that can be used in the synthesis of a EWG-activated benzylidene ligand is of high interest, as it shall lead to the significant reduction of synthetic and purification steps *en route* to an activated Hoveyda-Grubbs type catalyst.[16] Furthermore, if such building block is a part of the already existing large-scale industrial process, either as an intermediates or a side-product, its alternative way of utilization is welcomed, as it goes along with the recent policies of Circular Economy,[17] as well as with the general principles of green chemistry.[18]

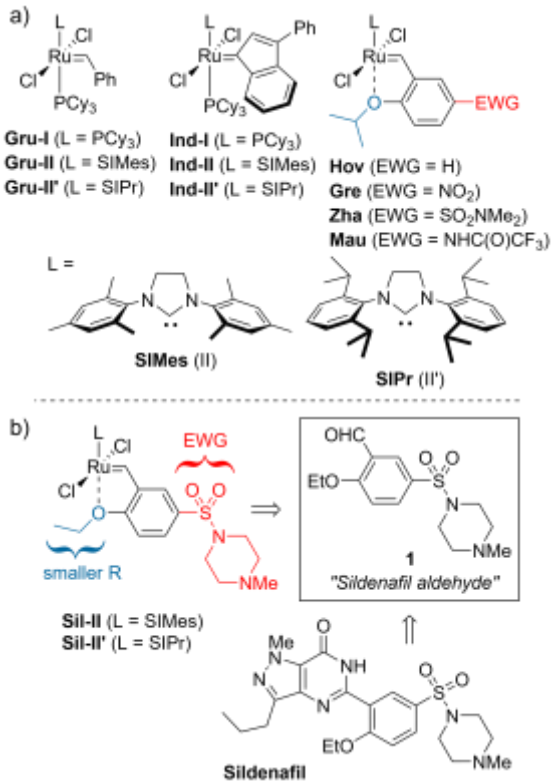

Figure 1. a) Selected NHC ligands ruthenium catalysts for olefin metathesis. b) New complex **Sil** derived from pharmaceutical building-block **1**. Cy = cyclohexyl.

Herein, we described the synthesis and the characterization of two new Hoveyda-Grubbs type 2nd generation olefin metathesis catalysts bearing a 2-ethoxy-5-sulfonamide-benzylidene ligand (**Sil-II** and **Sil-II'**, Figure 1b). These complexes have been obtained within only two simple steps from commercially available aldehyde **1,** a popular precursor in Sildenafil (Viagra™; Figure 1) production.[19]

Results and Discussion

Synthesis of the new EWG-activated Hoveyda-Grubbs type catalysts. Sildenafil (commercialized, among others, as Viagra™ by Pfizer or Maxigra™ by Polpharma) is a worldwide known inhibitor of phospho-diesterase(V) used in a treatment for erectile dysfunction[19c] and pulmonary arterial hypertension.[20] As an indication of the importance of this drug on the market, Viagra™ generated over 1 billion of US dollars worldwide for Pfizer in 2017.[21-22] The so-called *Sildenafil aldehyde* (**1**, Figure 1b), is a crucial intermediate in the convergent synthesis of this active pharmaceutical ingredient (API).[19a, 19b]

We realized that the same building block, widely available since it is used in a large-scale global manufacturing of Sildenafil, can be utilized as the precursor of choice in the synthesis of some new EWG-activated Hoveyda-Grubbs type catalysts (coded as **Sil-II** and **Sil-II'**, Figure 1b). Indeed, the EWG sulfonamide group in **1** is located in the required position, *para* to the ether fragment, exactly like in the other EWG-activated catalysts (Figure 1a). In addition, the presence of ethyl ether fragment in **1**, which is smaller than isopropyl ether (typically present in Hoveyda-Grubbs catalysts) shall activate the envisaged complex in metathesis by further destabilizing the catalyst resting state.[23]

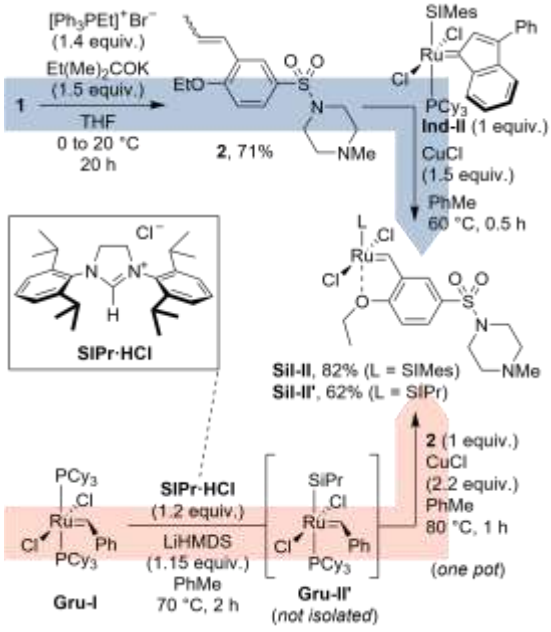

Scheme 1. Synthesis of complexes **Sil-II** and **Sil-II'** from **1** as a common precursor.

To reduce this hypothesis to reality, two complexes of general structure **Sil-II** and **Sil-II'** (with

SIMes and SIPr NHC ligands) were obtained from aldehyde **1** within only two simple synthetic steps, consisting of Wittig olefination reaction and ligand exchange. As illustrated in Scheme 1, styrene derivative **2** was obtained in good yield (71%) *via* the reaction of aldehyde **1** with ethyl(triphenyl)phosphonium bromide (1.4 equiv.) and potassium *tert*-pentoxide (1.5 equiv.) at 0 °C in THF for 20 h. The SIMes-bearing complex **Sil-II** was then obtained in good yield (82%) as a green microcrystalline solid *via* a stoichiometric metathesis reaction of **2** (1 equiv.) with the second-generation ruthenium-indenylidene complex **Ind-II**[24] (1 equiv.) in the presence of CuCl (1.5 equiv.) as phosphine scavenger.

A similar synthetic approach has been attempted for the preparation of the SIPr analogue, **Sil-II'**. Unfortunately, the use of the corresponding indenylidene complex (**Ind-II',** SIPr analogue of **Ind-II**) as a substrate did not provide a satisfying yield (<50%). Therefore, **Sil-II'** was conveniently synthesized from the *in situ* prepared second generation Grubbs complex **Gru-II'** (Scheme 1). The addition of the styrene derivatives **2** (1.0 equiv.) and CuCl (2.2 equiv.) followed by a simple column chromatography under atmospheric conditions and re-crystallization from a mixture of DCM and heptane gave the desired complex **Sil-II'** as a green microcrystalline solid (61% of yield). The required ruthenium source (**Gru-II'**) was prepared one pot from **Gru-I** and a free carbene (SIPr) made *in situ via* deprotonation of the corresponding chloride salt (SIPr·HCl) with hexamethyldisilazane lithium salt in toluene (LiHMDS). Of note, **Sil-II'** has been isolated as an ethyl acetate solvate (with one molecule of EtOAc) as confirmed by NMR, FTIR, and elemental analysis. For the sake of clarity, the solvation is omitted in the manuscript, however it was taken into account during the calculation of yields and catalyst loading.

X-ray solid-state structures. Crystals of the ruthenium complexes **Sil-II** and **Sil-II'** suitable for diffractometric measurements were obtained *via* liquid-to-liquid diff usion of heptane into concentrated DCM solutions of complexes. The structure of both derivatives was unambiguously confirmed by single-crystal X-Ray diffraction analysis (Figure 2). The investigated systems crystallize in monoclinic *C*2/c (**Sil-II**) and orthorhombic *Pbca* (**Sil-II'**) space group with one molecule of given compound in the asymmetric unit of the crystal lattice. In case of **Sil-II'**, the independent part of the unit cell contains also a molecule of heptane. The values of selected parameters describing the geometry of both compounds are reported in Table 1 along with those of other selected ruthenium SIMes[9, 25] and SIPr-based complexes.[13, 26] The crystallographic data and refinement details as well as a full set of bond lengths and values of valence and torsion angles for **Sil-II** and **Sil-II'** are given in Tables S11–S17 (ESI).

As expected, the Ru-atom of both analyzed complexes is penta-coordinated. The value of τ_5, which is a parameter characterizing the geometry of coordination centers of this type[27] is 0.32 and 0.26 for **Sil-II** and **Sil-II'** respectively. Therefore, the Ru(II) center, in both cases, adopts the symmetry closest to distorted square pyramid. Of interest, the reduction of the steric bulk on the alkoxy moiety in **Sil-II** does not affect the Ru–O bond length when compared to the one of **Hov-II** and **Gre-II** (Table 1). The value of this parameter is 2.269(5), 2.2562(10) and 2.2581(13) / 2.2869(12) Å for **Sil-II**, **Hov-II** and **Gre-II**, respectively. On the other hand, the corresponding bond within **Sil-II'** is noticeably shorter (2.2472(18) Å). In this case, the distance between the Ru and O atoms is comparable to the one reported for **Gre-II'** (2.244(2) Å) and slightly longer than in **Hov-II'** (2.2357(6) / 2.2490(6) Å). The values of Ru–C(NHC) bond length for **Sil-II** and **Sil-II'** are 1.981(7) and 1.973(3) Å, respectively and are similar to those noted for the most of SIMes or SIPr-based complexes compared in this study (Table 1). The only noteworthy difference is the Ru–C(NHC) bond of both **Sil-II** and **Sil-II'** being noticeably shorter than the one reported for **Mau-II'** complex (1.9911(13) Å). Comparison of the Ru=C(benzylidene) bond length in **Sil-II** and in **Sil-II'** (1.816(7) and 1.829(3) Å respectively) underline that the difference between them do not exceed a three-sigma criterion, and these mentioned values are in good agreement with those observed for other discussed derivatives (Table 1). The values of the Ru–Cl bond lengths in **Sil-II** (2.322(2) and 2.329(2) Å) as well as the one of **Sil-II'** (2.3335(7) and 2.3307(7) Å) do not differ from those reported for the vast majority of compared SIMes and SIPr complexes.

When analyzing the geometrical features of the first coordination sphere, special attention should be paid primarily on the Cl1–Ru–Cl2 and the C(NHC)–Ru–O valence angles, which can be considered as descriptors of the accessibility of the metallic center during the catalytic reaction. Of interest, the value of the Cl1–Ru–Cl2 in **Sil-II** and **Sil-II'** (respectively 158.32(9) and 157.25(2)°) are higher than those of the other complexes reported in Table 1. While the C(NHC)–Ru–O angle value of **Sil-II** (177(4)°) is similar to those reported for **Hov-II** and **Gre-II**, the values of these angles of all SIPr-based complexes reported in Table 1 are noticeably lower. These angles are ranging from 171.09(4) to 172.91(9)° and the highest value was observed for the **Sil-II'**.

Structural differences beyond the geometry of the coordination center of **Sil-II** and **Sil-II'** become more pronounced after respective alignment of their molecules. The superimposition of **Sil-II** and **Sil-II'** depicted in Figure 3 reveals that the molecular skeletons of these complexes exhibit different degree of deflection of the NHC relative to the plane of alkoxybenzylidene ligand. This feature was already highlighted by

10.1002/adsc.202100669

the different values of the O–Ru–C(NHC) valence angle (Table 1) and can also be described by the value of the angle between mean-planes of the NHC five-

10.1002/adsc.202100669

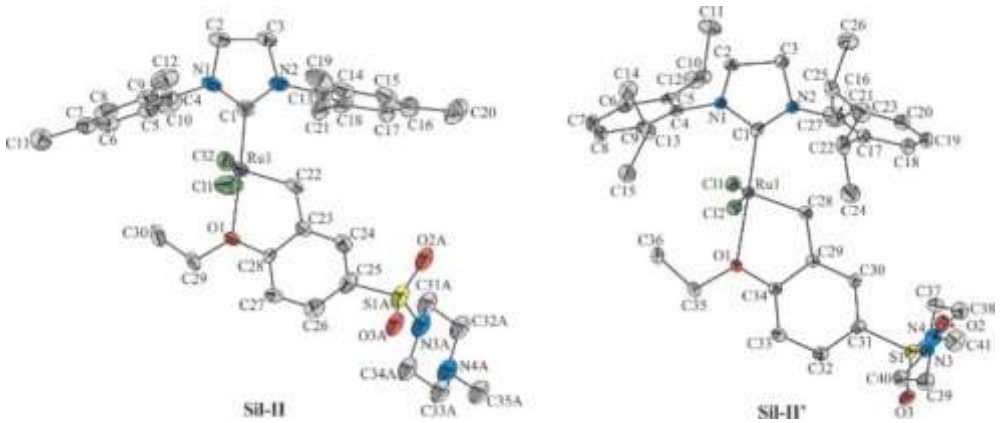

Figure 2. Molecular structure of **Sil-II** and **Sil-II'** complexes with crystallographic atom numbering. Displacement ellipsoids are drawn at the 50% probability level. The hydrogen atoms and minor component of disordered 4-methylpiperazine-1-sulfonyl moiety are omitted for clarity.

Table 1. Selected bond lengths [Å] and angles [°] for the Ru- based complexes **Sil**, **Gre**, **Hov** (SIMes and SIPr) and **Mau-II'**.

	SIMes Complexes		
	Sil-II	**Hov-II**[9]	**Gre-II** a) [25]
Ru–O	2.269(5)	2.2562(10)	2.2581(13)/2.2869(12)
Ru–Cl1	2.322(2)	2.3279(4)	2.3429(5) / 2.3330(5)
Ru–Cl2	2.329(2)	2.3380(4)	2.3272(5)/ 2.3299(5)
Ru–C(NHC)	1.981(7)	1.9791(15)	1.9827(18)/ 1.9790(19)
Ru=C(benzylidene)	1.816(7)	1.8286(15)	1.8286(19)/ 1.8251(19)
Cl1–Ru–Cl2	158.32(9)	156.251(15)	157.88(2) / 157.880(18)
C(NHC)–Ru–O	177.4(3)	176.06(5)	175.80(6) / 178.45(7)
	SIPr Complexes		
	Sil-II'	**Hov-II'** a) [26a]	**NG-II'**[26b]	**Mau-II'**[13]
Ru–O	2.2472(18)	2.2357(6)/2.2490(6)	2.244(2)	2.3002(10)
Ru–Cl1	2.3335(7)	2.3283(2)/2.3298(2)	2.3326(9)/	2.3293(4)
Ru–Cl2	2.3307(7)	2.3480(2)/2.3407(2)	2.3238(9)	2.3358(4)
Ru–C(NHC)	1.973(3)	1.9789(8) /1.9782(8)	1.985(3)	1.9911(13)
Ru=C(benzylidene)	1.829(3)	1.8322(8)/1.8307(8)	1.828(3)	1.8266(14)
Cl1–Ru–Cl2	157.25(2)	156.858(9)/155.881(8)	156.79(3)	153.478(14)
C(NHC)–Ru–O	172.91(9)	171.58(3)/171.88(3)	172.48(11)	171.09(4)

a) Crystals of these compounds contain two crystallographically independent molecules of given complex.

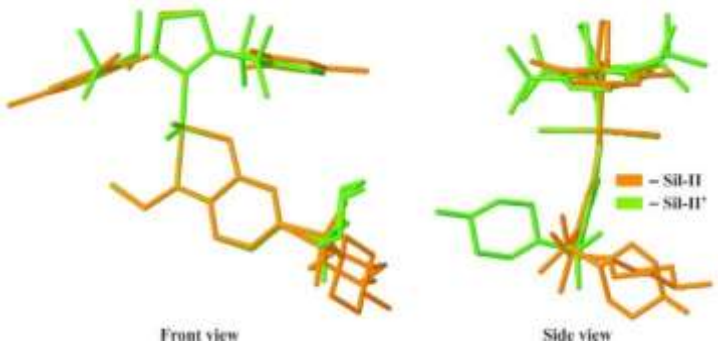

Figure 3. Superimposed molecules of **Sil-II** and **Sil-II'**. The hydrogen atoms are omitted for clarity.

membered ring and the phenyl ring of the benzylidene unit. These moieties in **Sil-II** and **Sil-II'** are inclined to themselves by the angle of 161.4(3) and 152.2(10) °, respectively. The substitution of the NHC moiety by the 2,6-disopropylphenyl groups (for SIPr in **Sil-II'**) results in noticeable twisting of this ancillary ligand on C2–C3 bond. Moreover, the investigated compounds differ in the spatial orientation of the substituents attached to the NHC. Indeed, the mean-planes of the aromatic rings defined by the C4–C10 and the C13–C18 atoms are inclined to the mean-plane of the five-membered ring by the angles of 88.4(3) and 89.5(3) ° for **Sil-II**, and 80.43(10) and 79.65(10) ° for **Sil-II'**. Finally, the 4-methylpiperazine-1-sulfonyl groups in **Sil-II** and **Sil-II'** are flipped on the opposite side of their alkoxybenzylidene units as depicted in the side view of Figure 3. In **Sil-II**, this functional group is additionally disordered.

Thermodynamic stability assessment. Despite their structural similarity, the two **Sil** catalysts were found to visibly differ in stability. Even during their preparations, it was easy to observe that **Sil-II** (SIMes complex) is sensitive towards air and moisture and its isolation in good yield requires a work-up under inert atmosphere as well as the use of a dry degassed solvent. In contrast, the SIPr variant, **Sil-II'**, could be isolated in air. The aforementioned difference in stability was not only observed during the synthesis and work-up process, but was also independently confirmed in stability tests conducted in dry degassed CD_2Cl_2 in a sealed NMR tube at 20 °C (Figure 4).

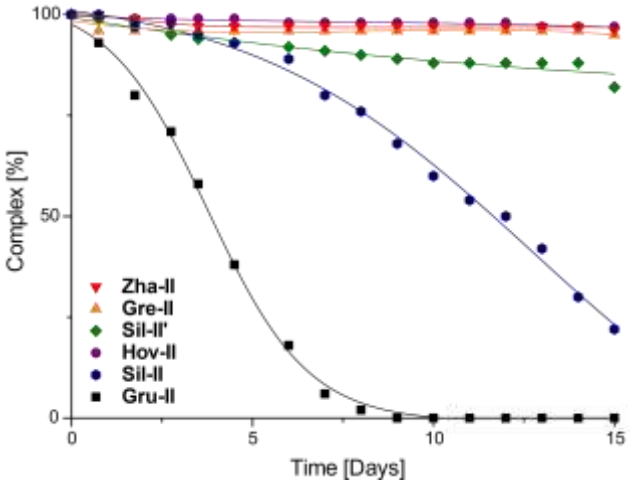

Figure 4. Curve of the stability of the catalysts in degassed DCM monitored by ^{1}H NMR **Hov-II** (purple), **Zha-II** (red), **Sil-II'** (green) and **Sil-II** (blue), **Gre-II** (orange) and **Gru-II** (black). Lines are visual aid only.

More than 20% of **Sil-II** decomposed within 7 days, while the SIPr complex **Sil-II'** exhibited only a small amount of decomposition after the same period of time. Notably, the latter complex reached only 12% of decomposition after twice-prolonged time (14 days in solution). In comparison, after 14 days in CD_2Cl_2 at room temperature, **Gre-II** (orange) and **Zha-II** (red) as well as **Hov-II** (purple) remained untouched (<5% of decomposition after 15 days). In contrast, the sensitivity of **Gru-II** (black) in solution is much more pronounced and led to the complete decomposition after 8 days within these conditions. The order of stability is thus as followed: **Gre-II** ≈ **Zha-II** ≈ **Hov-II**> **Sil-II'** > **Sil-II** > **Gru-II**. Of note, the SIPr analogue, **Sil-II'** could also be stored as a solid under argon for 3 months at room temperature without considerable loss (98% of the complex remaining).

Catalytic activity studies. The catalytic activity of **Sil** complexes was first tested in the ring closing metathesis (RCM) reaction of a standard model substrate, diethyl(diallyl)malonate (**3a**)[28] at 0.1 mol% catalyst loading (Figure 5). This well-known benchmark reaction unveiled that **Sil-II** initiated the reaction more quickly than the commercial **Zha-II** and **Hov-II** catalysts reaching 28% of conversion of **3a** within 5 min (k_{rel}(**Sil-II**) = 1.67)[29] in dichloromethane at 20 °C while after the same period of reaction time, complexes **Hov-II** and **Zha-II** led to 7 and 14% conversion, respectively within the same reaction conditions (k_{rel}(**Hov-II**) = 0.44 and k_{rel}(**Zha-II**) = 1.02). In contrast, nitro-substituted complex **Gre-II** exhibited a higher initiation rate for this reaction leading to a 38% conversion of **3a** within 5 min (k_{rel}(**Gre-II**) = 2.59). The relative rates of the RCM of **3a** were calculated with respect to the initial rate of RCM catalyzed by **Sil-II'** and led to k_{rel}(**Sil-II'**) = 1.0, k_{rel}(**Hov-II**) = 0.44, k_{rel}(**Zha-II**) = 1.02, and k_{rel}(**Gre-II**) = 2.59.
Thus, the order of the initiation rate of the reaction of RCM of compound **3a** is: **Gre-II** > **Sil-II** > **Sil-II'** ≈ **Zha-II** > **Hov-II**. Of note, this trend of reactivity follows the respective Hammett constants σ[30] as postulated by Blechert and co-workers[31] with values of $\sigma_{p,m}$(-NO_2) > $\sigma_{p,m}$(-SO_2(*N*-methylpiperazinyl)[32] ≈ $\sigma_{p,m}$(-SO_2NMe_2) > $\sigma_{p,m}$(-H). ((σ_p; σ_m) = (0.78; 0.71), (0.65; 0.51) and (0.00; 0.00) for -NO_2, -SO_2NMe_2 and -H respectively.
It is noteworthy that **Sil-II** exhibits a higher initiation rate than **Zha-II** catalyst, while the electronic properties (*i.e.* Hammett parameters) of their sulfonamide EWGs shall be similar. Such results are in accordance with the previous observations by Plenio *et al.* who demonstrated that the reduction of the steric bulk at the alkoxy moiety of the benzylidene ligand increased the initiation rate of RCM reactions.[33] Furthermore, the low stability of such alkoxy sterically unhindered complex is evenly in agreement with the literature.[11b, 23, 33] Importantly, increasing the bulk of the NHC in **Sil** (from SIMes to SIPr) seems to compensate the lack of

stability as well as the acceleration of activation rate of these catalysts since **Sil-II'** exhibit a similar k_{init} to **Zha-II** catalyst (k_{rel}(**Zha-II**) = 1.02). Albeit the initiation rates of these complexes are similar, the conversion of the RCM of **3a** catalyzed by **Sil-II'** surpassed the one promoted by **Zha-II** catalyst after 10 min of reaction and reached completion after 60 min (vs 90 min for **Zha-II**). In contrast, the **Sil-II**, exhibiting a higher initiation rate than **Sil-II'** and **Zha-II**, did not reach completion and led to a maximum conversion of 72%. Thus, the model RCM reaction results reflect the respective stability picture of these complexes.

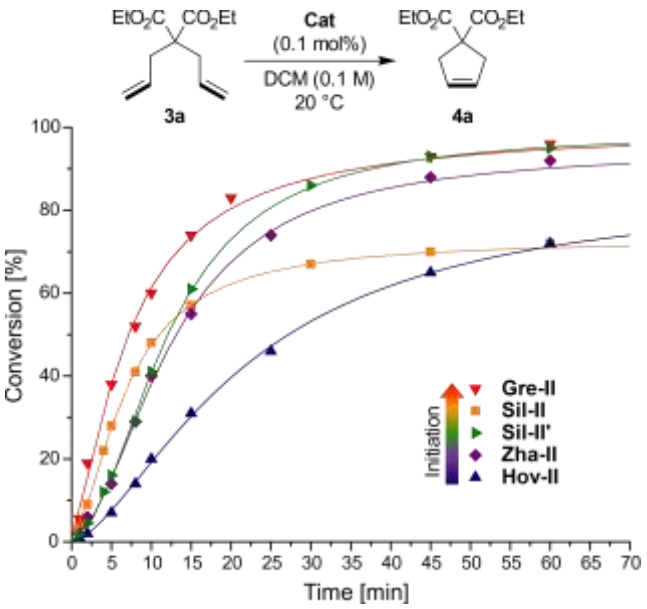

Figure 5. Plot of the reaction conversion in function of time for RCM of DEDAM (**3a**) (0.1 M) with commercially available SIMes-bearing catalysts and **Sil** (SIMes and SIPr) (0.1 mol %) in DCM at 20 °C: **Hov-II** (blue), **Zha-II** (purple), **Sil-II'** (green) and **Sil-II** (orange) and **Gre-II** (red). Conversion determined by NMR spectroscopy and confirmed by GC. Lines are visual aid only.

In order to have a proper comparison, the RCM reaction of **3a** was repeated with the SIPr-bearing Hoveyda-Grubbs catalysts under the same conditions (*i.e.* 0.1 mol% catalyst and 0.1 M **3a** in DCM at 20 °C; Figure 6). Again, the order of reactivity of the SIPr catalysts followed the trend of the Hammett parameters, namely **Gre-II'** > **Sil-II'** > **Mau-II'** > **Hov-II'** with relative initiation rate of 1.9, 1.0, 0.3 and 0.2 respectively (σ_p = 0.12, σ_m = 0.30 for -NHC(O)CF_3 substituent). Of note, while **Sil-II'** reached full conversion at the same time than the SIMes-bearing **Gre-II**, the SIPr derivative **Gre-II'** exhibited a higher productivity, reaching full conversion within 40 min (vs 60 min for **Gre-II** and **Sil-II'**). This behavior can be surprising since the initiation rate of **Gre-II** is higher than its SIPr analogue (k_{rel} 2.59 and 1.9 respectively). Nevertheless, this difference in activity can be explained by the lower stability of the active species (*i.e.* methylidene complex) generated from **Gre-II** compared to **Gre-II'**. This lower stability of the active complex induces an early inflexion point of the curve (*c.a.* 15 min) and consequently a longer reaction time to reach completion.

Similar picture has been obtained for another benchmark reaction[28]—RCM of *N*,*N*-diallyltosylamide (**3b**) in DCM (0.1 M) using catalyst loading of 0.1 mol%, underlining the same order of relative initiation rates for **Hov-II'**, **Mau-II'**, **Sil-II'** and **Gre-II'** which were 0.1, 0.4, 1.0 and 1.5 respectively (vs 0.2, 0.3, 1.0 and 1.9 respectively, noted for RCM of **3a**, (see ESI, Scheme S9).

Because the above experiments witnessed that the SIMes bearing catalyst **Sil-II** is visibly inferior to its SIPr analogue **Sil-II'** in terms of productivity and stability, for further studies we decided to focus on the latter.

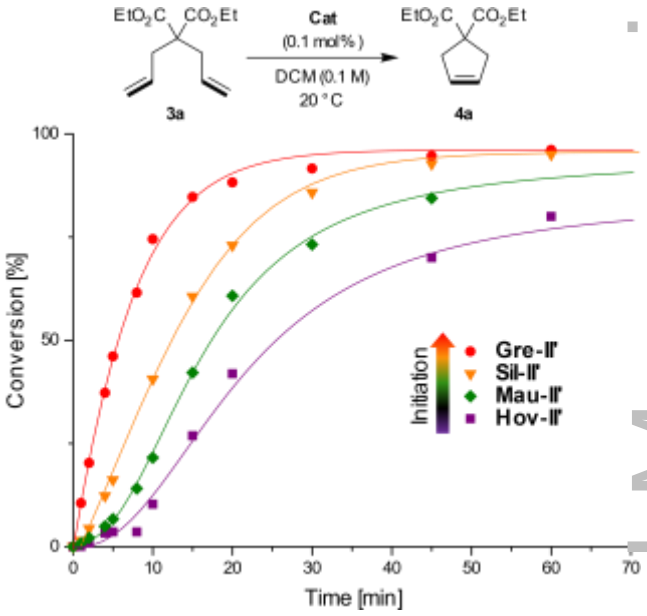

Figure 6. Plot of the reaction conversion in function of time for RCM of DEDAM (**3a**) (0.1 M) with commercially available SIPr-bearing catalysts and **Sil-II'** (0.1 mol %) in DCM at 20 °C: **Hov-II'** (purple), **Mau-II'** (green), **Sil-II'** (orange) and **Gre-II'** (red). Conversion determined by NMR spectroscopy and confirmed by GC. Lines are visual aid only.

Scope and limitation study. The application profile of the more robust **Sil-II'** catalyst was evaluated with a set of diene derivatives **3a**-**3h** under mild conditions (Ru loading of only 0.1 mol%, ambient temperature, 2 h of reaction time; Scheme 2). The relatively structurally undemanding 5- and 6-membered carbo- and heterocycles **4a**-**4f** featuring di- and trisubstituted C–C double bonds were formed in good to quantitative yields at 20 °C. Gratifyingly, the spirocyclic anthrone derivative (**4g**) was formed in high yield (97%). Furthermore, the more densely functionalized barbituric acid derivative **4h** was formed in high yield under similar mild conditions (Scheme 2).

Next, the application profile of **Sil-II'** has been probed in the cross- metathesis (CM) reaction (Scheme 3). To

do so, we started with a benchmark CM reaction[28] between allylbenzene (**5**) and (*Z*)-1,4-diacetoxybutene (**6**) in DCM at 20 °C. Within 1 h, alkene **5** was completely transformed into the corresponding CM product **7**, which has been isolated with 85% yield and *E*/*Z* ratio of 76/24. It is noteworthy that isomerization of allylbenzene **5** to the corresponding styrene was not observed during the reaction.[34] Next, electron deficient CM partners, such as α,β- unsaturated ester (**9**), ketone (**11**),[35] and sulfonamide (**14**)[36] were tested. These compounds are known to be challenging partners in CM reactions (Type II and III olefins)[37] because the C–C double bond in these compounds is less reactive in metathesis due to the conjugation with the EWG-group.[37-38] Nevertheless, the reaction of terminal alkene **8** with **9** and **11** occurred in the presence of 0.5 mol% of **Sil-II'** in DCM within only 2 h at 20 °C to afford the corresponding α,β- unsaturated carbonyl compounds **10** and **12** with good yields (78 and 84%, respectively). This attainment led us to consider even more challenging vinyl sulfonamide **14** as a partner in CM reaction with indole derivative **13**, which has been previously reported[36] as the key step in the synthesis of a naratriptan derivative **15**.[39]

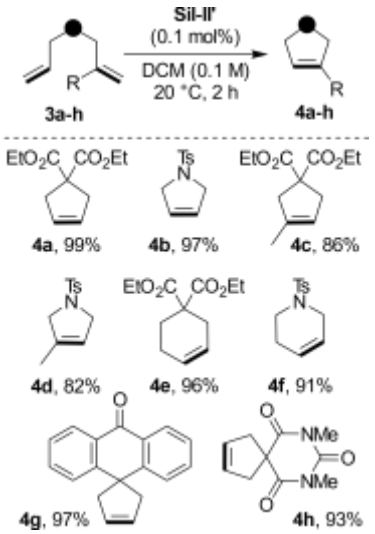

Scheme 2. RCM reactions of model dienes catalyzed by **Sil-II'** (isolated yields of analytically pure substances).

In this report, the cross-coupling between **13** and **14** was achieved with a relatively high loading (5 mol%) of **Gre-II** at 30 °C within 3 h to yield to compound **15** in 72%.[36]

Relying on the observed high stability of SIPr-based **Sil-II'** and its longevity in reaction mixture (*vide infra*), the CM of the indole **13** and the sulfonamide **14** was undertaken with only 0.2 mol% of **Sil-II'** at ambient temperature (20 °C). Satisfyingly, even such mild reaction conditions allowed the isolation of the product **15** in a good yield of 85% within 15 h (Scheme 3). The encouraging results obtained so far with **Sil-II'** led us to approach even more complex polyfunctional products relevant to the pharmaceutical industry. To that aim, *N*,*N*-diallylsulfonamide derivative of Sildenafil **16** was subjected to RCM in DCM (Scheme 4). Despite the high level of functionalization of this molecule and the presence of the acidic proton of the pyrazolopyrimidinone moiety, the RCM of diene **16** reached completion within 0.5 h at 20 °C in the presence of only 0.5 mol% of **Sil-II'**. Of note, product **17** was found to be slightly soluble in cold DCM. Therefore, filtration of the cooled reaction mixture (0 °C) and the subsequent washing of the resulting solid with cold DCM enabled the isolation of the desired product (92%) with a low content of Ru contamination of 9.3 ppm.

Next, the precursor of Pacritinib **18** was selected as a more challenging substrate for the RCM reaction. Pacritinib is of particular interest because of potential pharmaceutical applications for the treatment of myelofibrosis and lymphoma. From a chemical point of view, compound **18** is a rather problematic substrate for RCM mainly due to the presence of chelating sites, such as basic nitrogen atoms present on the amino-pyrimidine fragment that are able to "arrest" the catalyst in the form of a stable chelate. Moreover, **18** possesses two labile *O*-allyl fragments that create the risk of C–C double bond isomerization (shift).[37, 40] Therefore, the RCM macrocyclization of this diene shall be considered as a rather challenging transformation. The group of Williams in 2011 reported the RCM of diene **18** (1 mM) in acidic conditions (aqueous HCl, pH ≈ 2.0-2.2) in DCM using 10 mol% of **Gru-II** as the catalyst.[41] Under such conditions, the RCM reaction at 40-45 °C afforded product **19** in 74% with an *E*/*Z* ratio of 85/15.

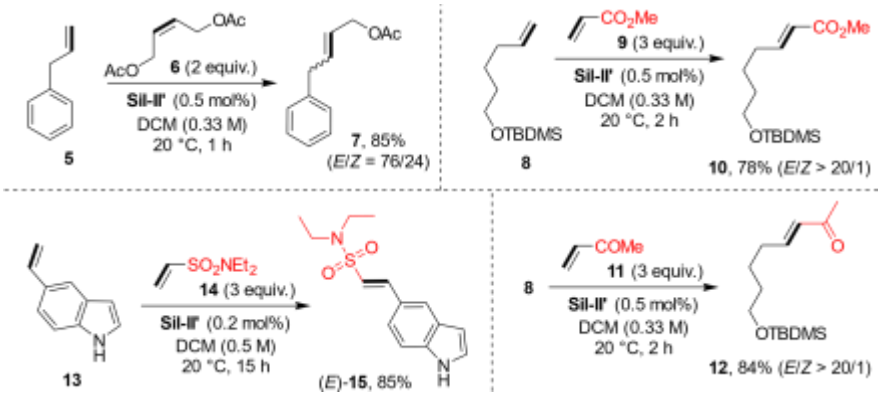

Scheme 3. Model CM reactions catalyzed by **Sil-II'** at ambient temperature (isolated yields of analytically pure substances). TBDMS = *tert*-butyldimethylsilyl.

10.1002/adsc.202100669

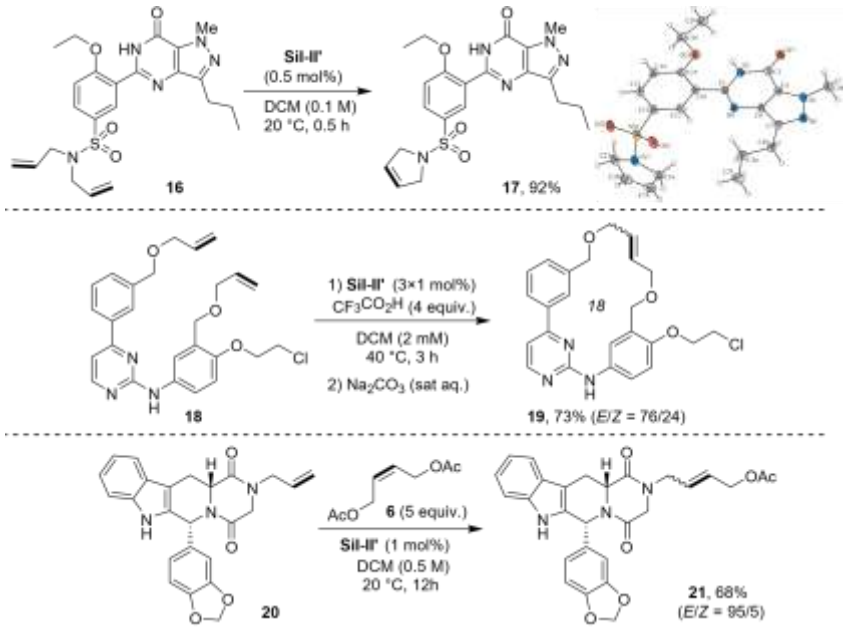

Scheme 4. Metathesis reactions of APIs **16**, **18** and **20** catalyzed by **Sil-II'** (isolated yields of analytically pure substances) and the solid-state structure of the **17**.

In 2017, Hoveyda and co-workers disclosed the preparation of Pacritinib precursor **19** using an *E*-selective molybdenum-based metathesis catalyst.[42] In this reaction, the boryl-protected diene (20 mM in dry toluene) was treated at 22 °C with 10 mol% of the catalyst to yield the Pacritinib precursor **19** (73%) with the *E*/*Z* ratio of 92/8. Despite the high selectivity of this reaction, the protection of the NH group with a *tert*-butoxycarbonyle group (Boc) of the pyrimidine moiety was required to reach an acceptable yield (34% yield of **19** in the case of the nonprotected derivative) which force additional synthetic steps to obtain the target molecule Pacritinib.

Based on the above reports, the macrocyclization of compound **18** (2 mM in DCM) was undertaken in the presence of triflic acid (4 equiv.) to protonate the basic nitrogen sites present in the substrate. Remarkably, with **Sil-II'** catalyst, the full conversion was reached after 3 h of reflux (45 °C), using a relatively low catalyst loading of 3×1 mol% (the catalyst was added portion wise during the reaction). The macrocycle **19** was isolated in 73% yield (*E*/*Z* = 76/24) after a basic work-up with saturated Na_2CO_3 and column chromatography on silica gel (Scheme 4).

The final example of a polyfunctional molecule of pharmaceutical interest used in this study was a Tadalafil derivative.[19a] Tadalafil is a potent inhibitor of phosphodiesterase(V) used as the same purpose than Sildenafil (treatment of erectile dysfunction) and commercialized as Cialis™ by Lilly Eli & Company.[43] In contrast to Sildenafil-related diene **16**, *N*-allyl Tadalafil derivative **20** proved to be more reluctant in metathesis. Nevertheless, with 1 mol% of **Sil-II'**, the uneventful CM reaction between **20** and (*Z*)-1,4-diacetoxybutene (**6**, 5 equiv.) occurred at 20 °C to afford the expected product **21** in 68% yield with a relatively high *E*/*Z* ratio of 95/5.

Assessing the practicability: Applicability in non-degassed solvent and Ru removal after the reaction. Until now, all experiments have been conducted in dry and degassed DCM (3 ppm of water), under protective atmosphere. However, one of the key features of Ru metathesis catalysts is there uses under air and in not strictly dry solvents, which can be beneficial in practical industrial setups.[44] To further investigate the applicability of **Sil-II'** in such non-perfect conditions, we attempted RCM of **3a** in a non-dry and non-degassed DCM (the water content in the solvent was 265 ppm according to Karl Fisher titration). Under such conditions 0.5 mol% of **Sil-II'** reached 95% of conversion after 3 h. In the case of **Gre-II'** and **Hov-II'**, the RCM reaction of **3a** led to full conversion (>99%). Interestingly, the SIMes bearing **Gre-II** led to only 69% of conversion after 3 h (Scheme 5). This result demonstrated the generally higher stability of the SIPr catalysts during the metathesis reaction.

We also attempted to check if the new complex, **Sil-II'**, leads to similar Ru contamination levels as other catalysts of the Hoveyda-Grubbs family. To do so, samples of crude product **4a** obtained in the above test reactions were used to determine such Ru contamination (Scheme 5). Of note, in contrast to product **17** which could be filtered off the reaction mixture, the purification of the oily product **4a** is more challenging and required the addition of Ru scavenger such as isocyanide **22**.[45] Therefore, the crude reaction mixtures of scheme 5 were stirred with commercial scavenger **22** and silica gel in DCM at ambient temperature for 30 min and then filtered. After this simple phase separation procedure,[46] the content of Ru was measured by ICP-MS, showing similar levels (24-66 ppm) of trace Ru contamination in **4a** for all Hoveyda-Grubbs catalysts tested.

10.1002/adsc.202100669

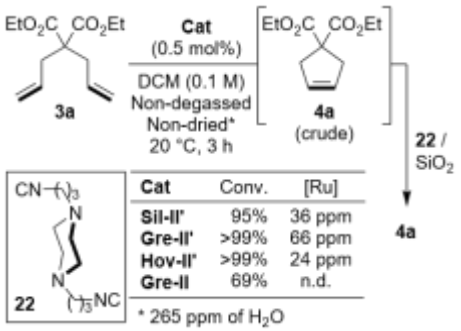

Scheme 5. RCM of **3a** catalyzed by selected SIPr-bearing catalysts in non-dried and non-degassed DCM (265 ppm of water) and purification of **4a** from spend catalyst traces. n.d. = non-determined

Use in green solvents. As pointed out recently by Sherwood, the use of chlorinated solvents soon will be banned (or are already prohibited) and the society of chemists must adapt to.[47] Therefore, we decided to investigate the application profile of **Sil-II'** in greener and more sustainable solvents than DCM. A set of environmentally friendly solvents, composed of 2-methyltetrahydrofuran (2-MeTHF), cyclopentyl methyl ether (CPME), anisole, ethyl acetate (AcOEt), dimethyl carbonate (DMC) and acetone, has been selected according to the CHEM21 selection guide of solvents.[48] The activity of **Sil-II'** in these beforehand dried and distilled solvents has been checked using the model RCM reaction of **3a** under the same conditions as used previously, namely 1 mmol of **3a** (0.1 M), 0.1 mol% of the catalyst at 20 °C under inert atmosphere, and the results are depicted in Figure 7. Surprisingly, the ethereal solvents such as 2-MeTHF, CPME, or anisole were found to be deleterious for the RCM of **3a** with a relative initiation rate of k_{rel}(2-MeTHF) = 0.03, k_{rel}(CPME) = 0.24 and k_{rel}(anisole) = 0.34 (with respect to the initiation of the reaction in DCM which was $4.8.10^{-5}$ mol·s^{-1}). Surprisingly, the use of AcOEt also decreased the efficiency of **Sil-II'**, resulting in a slow initiation comparable to CPME (k_{rel}(AcOEt) = 0.28). Nevertheless, the other carbonyl group-containing solvents such as DMC or acetone offered higher initiation rate than the ethereal solvents and AcOEt with relative initiation rate of k_{rel}(DMC) = 0.84 and k_{rel}(acetone) = 1.19.

For further studies acetone was selected, as it allowed to achieve both high initiation rate and good overall productivity. To provide cogent evidence for the applicability of the new catalyst in this solvent, the RCM reaction of Sildenafil derivative **16** was undertaken. While diene **16** proved to be poorly soluble in acetone, the RCM reaction uneventfully occurred at 20 °C in the presence of 0.5 mol% of **Sil-II'** giving product **17** in 94% of yield (Scheme 6). The only difference between this reaction and the RCM previously made in DCM is the longer reaction time (2 h, 94% of yield *vs* 0.5 h, 92% yield for DCM, see Scheme 4).

In contrast to the reaction in DCM, the metathesis product **17** was highly insoluble in acetone and precipitated during the reaction allowing the isolation of analytically pure product **17** in 94% yield within a simple filtration without any cooling required. Of high interest, this simple filtration led the recovery of product **17** with a very low ruthenium contamination content of only 3.9 ppm (vs 9.3 with DCM).

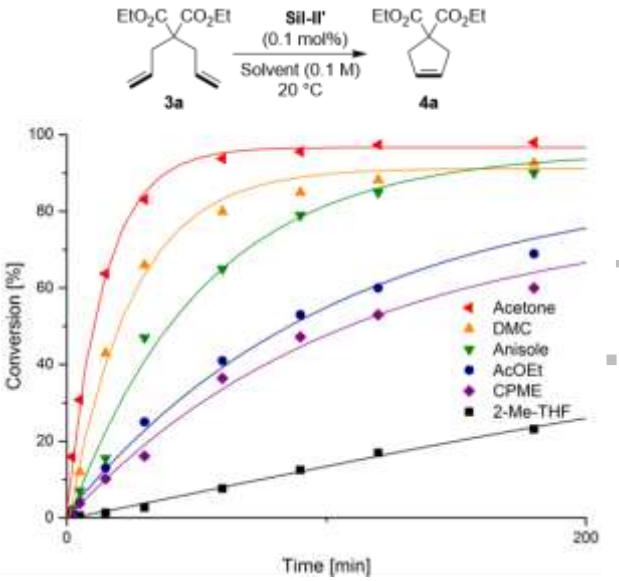

Figure 7. Plot of the reaction conversion in function of time for RCM of **3a** (0.1 M) in different solvents catalyzed by **Sil-II'** (0.1 mol %) at 20 °C: 2-MeTHF (black), CPME (purple), AcOEt (blue), anisole (green), DMC (orange), and acetone (red). Conversion determined by ^{1}H NMR spectroscopy and confirmed by GC. Lines are visual aid only.

The second complex substrate of medicinal chemistry context, *N*-allyl Tadalafil derivative **20** was also almost completely insoluble in acetone. In contrast to substrate **16**, no metathesis was observed in the presence of 1 mol% of **Sil-II'** at room temperature. Heating the reaction mixture to reflux (*c.a.* 60 °C) led to the complete dissolution of the substrate and the CM reaction with 5 equiv. of (*Z*)-1,4-diacetoxybutene (**6**) within 3 h afforded product **21** in 73% yield (*E*/*Z* ratio: 92/8; comparing with 68% of yield in DCM, see Scheme 4).

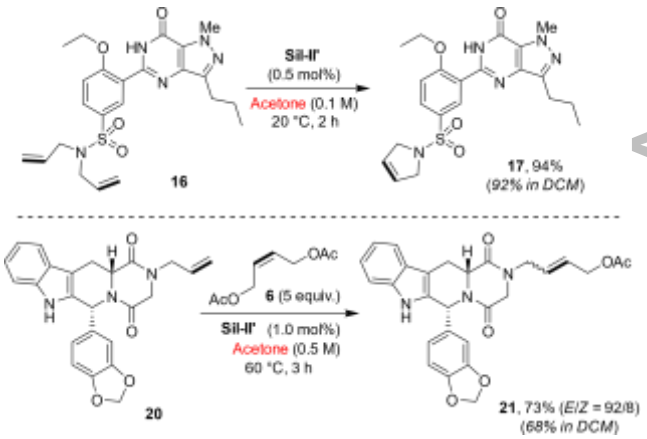

Scheme 6. Metathesis of pharmaceutical relevant compounds **16** and **20** catalyzed by **Sil-II'** in acetone (isolated yields of analytically pure substances).

Mechanism of the Sil-II' initiation.

In order to gain information on the mechanism of activation of the SIPr-catalysts used in this study (depicted in Figure 8) and, in particular, to check the possible influence of the ethoxy chelating moiety of **Sil-II'** on this mechanism, kinetic evaluations were conducted using a model diene **3a**[49] in DCM utilizing time-dependent UV-VIS spectroscopy according to the procedure described by Plenio and co-workers,[33] *i.e.* monitoring the evolution of the absorbance (at the peak of maximal absorption for each catalysts) as a function of time which lead to the determination of k_{obs}(Ru-SIPr) according to the kinetic model in equation 1.[50]

$$v = -\frac{d[\boldsymbol{RuII'}]}{dt} = k_{obs}*[\boldsymbol{RuII'}] \quad \text{(eq 1)}$$

The activation parameters of the rate determining step (RDS) of the initiation mechanism, namely, activation energy (Ea), entropy ($\Delta H^{\ddagger}$), enthalpy ($\Delta S^{\ddagger}$), and Gibbs free energy ($\Delta G^{\ddagger}$), were obtained for each pre-catalyst and reported in Table 2. Gratifyingly, the activation energies (E_a) as well as the Gibbs free energies of the rate determining step of the pre-catalysts activation reflect the trend of reaction rate observed in Figure 6, namely **Gre-II'** > **Sil-II'** > **Mau-II'** > **Hov-II'** with respective values of E_a of 9.1 kcal·mol^{-1}, 13.2 kcal·mol^{-1}, 17.7 kcal·mol^{-1}, and 21.8 kcal·mol^{-1} and $\Delta G^{\ddagger}$ values of 20.2 kcal·mol^{-1}, 20.6 kcal·mol^{-1}, 21.0 kcal·mol^{-1}, 22.5 kcal·mol^{-1}. Enthalpy and entropy values were found to be more disparate with values ranging from 8.4 to 21.2 kcal·mol^{-1}for $\Delta H^{\ddagger}$ and from -18.1 to -167.1 J·mol^{-1}·K^{-1} for $\Delta S^{\ddagger}$. The small value of entropy of **Hov-II'** (-18.1 J·mol^{-1}·K^{-1}) indicates that the number of degrees of freedom of the RDS does not change significantly from the initial state of the reaction which could be explained by the absence of the coordination of the olefin to the ruthenium center at the RDS. Combined with the important $\Delta H^{\ddagger}$ (**Hov-II'**) parameter, these results would suggest that the activation mechanism of **Hov-II'** is purely dissociative. (Figure 8) The high negative entropy values $\Delta S^{\ddagger}$ in the other cases, *i.e.* -167.1, -108.3, and -130.4 J·mol^{-1}·K^{-1} for **Gre-II'**, **Sil-II'** and **Mau-II'** respectively, do not exclude the dissociative pathway as the activation mechanism of these pre-catalysts but only indicates a significant contribution of the step of the coordination of the olefin to the ruthenium center on the RDS (*i.e.* contribution of k_1, figure 8). Therefore, it is impossible to conclude on the mechanism type of the three latter systems relying only on these activation parameters.

Consequently, further mechanistic investigations were required to elucidate the initiation mechanisms of these three catalysts. To do so, UV-visible spectroscopy was employed to evaluate the evolution of k_{obs} (defined in eq. 1) of the SIPr systems under second and pseudo first-order conditions ([**3a**] >> [Ru]) as a function of the concentration of **3a** (from 0.03 – 2 M). The Plenio's group elegantly demonstrated that the dependence of k_{obs} on olefin concentration allows the differentiation between the activation mechanisms of the respective catalysts. In the case of a dissociative mechanism, the corresponding fit of k_{obs}-[olefin] plot is a hyperbolic function defined by eq. 2. From a theoretical point of view, such definition of k_{obs} is the result of the combination of a two-step reaction involving a limiting pre-equilibrium *i.e.*, $k_d << k_{-d}$ and $k_d << k_1$.[51] (Figure 8 and see demonstration in ESI)

$$k_{obs} = \frac{k_d * \frac{k_1}{k_{-d}}[\boldsymbol{3a}]}{(1+\frac{k_1}{k_{-d}}*[\boldsymbol{3a}])} \text{ (eq. 2)} \qquad k_{obs}=k_2*[\boldsymbol{3a}] \text{ (eq. 3)}$$

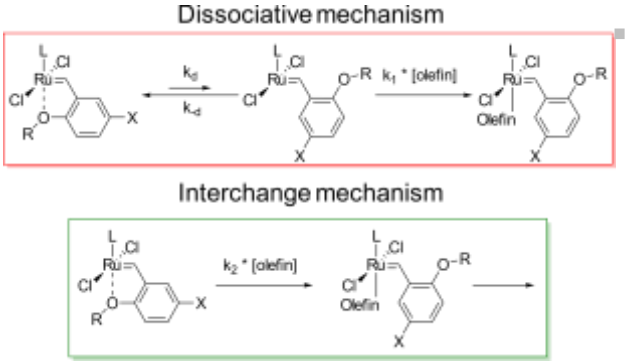

Figure 8. Two possible mechanisms of Hoveyda-Grubbs catalyst initiation: interchange and dissociative.

Table 2. Activation parameters (obtained for [**3a**] = 0.66 M, [Ru] = 10^{-4} M) and kinetic parameters for the initiation of complexes **Gre-II'**, **Sil-II'**, **Mau-II'** and **Hov-II'** with **3a**.

	Activation Parameters			
	E_a (kcal/mol)	**$\Delta H^{\ddagger}$** (kcal/mol)	**$\Delta S^{\ddagger}$** (J/mol/K)	**$\Delta G^{\ddagger}$** (kcal/mol)
Gre-II'	9.1 ± 0.3	8.4 ± 0.4	-167.1± 5.3	20.2 ± 1.1
Sil-II'	13.2 ± 1.3	13.0 ± 0.6	-108.3 ± 8.9	20.6 ± 0.9
Mau-II'	17.7 ± 1.4	11.9 ± 1.4	-130.4 ± 19.9	21.0 ± 0.9
Hov-II'	21.8 ± 1.8	21.2 ± 3.2	-18.1 ± 44.1	22.5 ± 6.4
	Kinetic Parameters			
	k_d ($s^{-1}\cdot10^{-3}$)	**k_2** (L/mol/s·10^{-3})		
Gre-II'	34.9 ± 9.9	-		
Sil-II'	-	4.3		
Mau-II'	3.4 ± 0.9	-		
Hov-II'	0.6± 0.3	-		

On the other hand, a linear fitting of the plot of k_{obs}- [olefin] would indicate that the activation mechanism of the catalysts involves an associative interchange (I_a) pathway. In the latter case, the slope of the fit determines k_2 of the interchange pathway as defined in eq. 3 (see Figure 8). Finally, it is plausible in some cases that both pathways *i.e.* dissociation and interchange, intervene in the initiation mechanism. In such

case, the fit of the plot of k_{obs}-[olefin] would be defined by the combination of the two equations such as k_{obs} = eq. 2 + eq. 3. The experiments previously described were thus carried out for each catalyst (at a concentration of 10^{-4} M) with **3a** (from 0.03 to 2 M) in CD_2Cl_2 at 20 °C. The respective data obtained are reported in Figure 9. Gratifyingly, the k_{obs} *vs* [**3a**] of **Hov-II'** were fitted satisfactorily with the hyperbolic function of eq. 2 which is confirming the dissociative pathway of this catalyst. The same behavior of k_{obs} was observed for **Gre-II'** and **Mau-II'** and the resulting fits correspond to a hyperbola. Importantly, the attempt to fit these plots with eq. 2 + eq. 3 did not converge to a satisfactory set of parameters indicating a purely dissociative pathway for these three pre-catalysts. The value of the dissociation rate constant k_d for these complexes could thereby be determined as $0.6 \cdot 10^{-3}$, $3.4 \cdot 10^{-3}$, and $34 \cdot 10^{-3}$ s^{-1} for **Hov-II'**, **Mau-II'** and **Gre-II'** respectively.

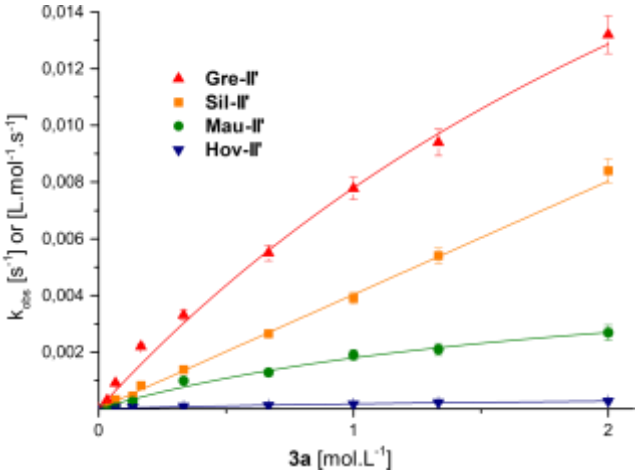

Figure 9. Plot of k_{obs} *vs* [**3a**] for complexes **Gre-II'** (red), **Sil-II'** (orange), **Mau-II'** (green) and **Hov-II'** (blue). Lines correspond to the hyperbolic fit of the data according to eq. 2 (dissociative pathway) for **Gre-II'**, **Mau-II'** and **Hov-II'** and to a linear fit for **Sil-II'** (interchange mechanism).

The attempt to fit the dependencies of k_{obs}(**Sil-II'**) on [**3a**] with eq. 2 led to aberrant values of the parameters ($k_d > 10^{12}$ s^{-1}) and showed an important deviation of the fit residuals. These data appeared to be best fitted with a linear function such as eq. 3. These results point out that the mechanism of initiation of the pre-catalyst is a pure interchange (associative type) one. Thus, we can extract the value of k_2 which $4.8 \cdot 10^{-3}$ $L \cdot mol^{-1} \cdot s^{-1}$.

Since the electronic properties of the EWG of **Sil-II'** are comprised between those of **Hov-II'** and **NG-II'** (H and NO_2 respectively), we can assume that the change of the initiation mechanism is mainly relying on the decrease of the steric congestion of the alkoxy moiety. Such behavior is reminiscent with the observation of the group of Plenio evaluating the effect of MeO-substituted benzylidene derivatives of **Gre-II** and **Hov-II** on the mechanism of activation. What is striking in the case of **Sil-II'** is that the small decrease of the steric bulk at the alkoxy moiety (-O*i*Pr to -OEt) impacts dramatically the mechanism of activation when compared to its SIPr-counterpart.

Conclusion

We have shown that large-scale produced API (active pharmaceutical ingredient) precursor, *sildenafil aldehyde*, can be used as a convenient starting material in the preparation of EWG-activated Hoveyda-Grubbs type ruthenium olefin metathesis catalysts. Stability and catalytic activity tests disclosed that the smaller NHC-ligand bearing complex (**Sil-II**, with SIMes ligand) is visibly less stable and productive than its analogue, **Sil-II'**, featuring bulkier NHC SIPr ligand. Good application profile of the latter catalyst was confirmed in a set of diverse metathesis reactions including ring-closing (RCM) and cross-metathesis (CM) of both model substrates and complex polyfunctional pharmaceutical building-blocks, including a challenging macrocyclization of Pacritinib precursor. Compatibility of the new catalyst with various green solvents selected according to the CHEM21 guide was checked and the metathesis reactions of Sildenafil and Tadalafil-based substrates were successfully conducted in acetone, showing that the new catalyst may be used in green pharmaceutical production. The mechanism of **Sil-II'** initiation has been investigated through kinetic experiments and the obtained results unveiled that the decrease of the steric hindrance of the chelating alkoxy moiety (from *i*PrO to EtO) favors the interchange initiation pathway over the dissociation pathway typical for other 2nd generation Hoveyda-Grubbs catalysts. We believe that the reported results may be not only to interest of chemists applying olefin metathesis in organic synthesis, but also useful for organometallic chemistry experts designing new ruthenium-based catalysts.

Experimental Section

Unless otherwise noted, all materials were purchased from commercial suppliers and used as received. All reactions requiring exclusion of oxygen and moisture were carried out in dry glassware with dry solvents (purified using *MBraun* SPS) under a dry and oxygen-free atmosphere using Schlenk technique. The bottles with ruthenium catalysts were stored under argon atmosphere, but no special precautions were taken to avoid air or moisture exposure in the moment of extracting catalysts from the bottles. NMR (^1H and ^{13}C) spectra were recorded on *Agilent* Mercury 400 MHz spectrometer at ambient temperature with $CDCl_3$ or CD_2Cl_2 used as a solvent. GC measurements were carried out using *PerkinElmer Clarus 580* employing InertCap 5MS-Sil column and helium as a carrier gas. IR spectra were recorded using JASCO FT/IR-6200 spectrometer. The substances were examined as a film or in the solution. Wavenumbers ($\tilde{\upsilon}$) are reported in cm^{-1}. The obtained data was processed with the software Omni32. UV-Vis spectra were recorded using *Thermo Fischer Scientific Evolution* 300 UV-Vis spectrophotometer in 10.00 mm QS cuvettes. Wavelenghts (λ) are reported in nanometres (nm), whereas absorbance (A) is given in absorbance units (a.u.). Scan speed was set to 600 nm/min, range 300 – 500 nm, bandwidth 1 nm and data interval 1 nm. HRMS measurements were carried out using

AutoSpec Premier spectrometer. Elemental Analysis were carried out at the Polish Academy of Science, Institute of Organic Chemistry. ICP-MS: Ruthenium content was determined using *NexION 300D* apparatus (*Perkin Elmer*, USA). Column Chromatography was performed using *Merck* Millipore silica gel (60, particle size 0.043 – 0.063 nm). TLC was performed using Merck Silica Gel 60 F_{254} precoated aluminium sheets. Substances were visualised using UV-light (254 or 365 nm) or by stains after $KMnO_4/K_2CO_3$/NaOH reagent treatment (aqueous solution)

1-((4-ethoxy-3-(prop-1-en-1-yl)phenyl)sulfonyl)-4-methylpiperazine (Styrene 2):
To a suspension of ethyltriphenylphosphonium bromide (5.25 g, 14 mmol, 1.4 equiv.) in THF (30 mL), a solution of potassium *tert*-pentoxide (25% in toluene, 7.57 g, 15 mmol, 1.5 equiv.) was added dropwise. The resulting orange mixture was stirred at room temperature for 30 min. Then, the mixture was cooled down to 0 °C and a solution of aldehyde **1** (3.12 g, 10 mmol, 1 equiv.) in THF (10 mL) was added dropwise. The reaction mixture was stirred at 0 °C for 15 min, then was allowed to warm up to room temperature and was stirred for 20 h. The reaction was quenched with a saturated aqueous solution of NH_4Cl (3 mL) and then extracted with EtOAc (3 x 5 mL). The combined organic layers were washed with brine (5 mL), and dried over anhydrous $MgSO_4$. Solids were filtered out and all the volatiles were removed under reduced pressure to afford crude product **2** which was then purified using column chromatography (stationary phase: Al_2O_3, eluent: EtOAc/*n*-hexane from 20:80 to 40:60 v/v). The product was obtained as a white solid (1.55 g, 71%, *E*/*Z* = 88/12). **^{1}H NMR (400 MHz, $CDCl_3$) δ:** 7.72 (d, *J* = 2.3 Hz, 1H), 7.54 (dd, *J* = 8.6, 2.3 Hz, 1H), 6.89 (d, *J* = 8.7 Hz, 1H), 6.67 (dq, *J* = 15.8, 1.5 Hz, 1H), 6.30 (dq, *J* = 15.9, 6.6 Hz, 1H), 4.10 (q, *J* = 7.0 Hz, 2H), 3.02 (bs, 4H), 2.47 (t, *J* = 4.8 Hz, 4H), 2.26 (s, 4H), 1.91 (dd, *J* = 6.7, 1.7 Hz, 3H), 1.48 (t, *J* = 7.0 Hz, 3H). **^{13}C NMR (101 MHz, $CDCl_3$) δ:** 158.8, 128.8, 128.3, 127.8, 126.4, 126.0, 124.4, 111.2, 64.2, 54.0, 46.0, 45.7, 18.9, 14.7. **FT-IR (CH_2Cl_2 film):** 3040, 2979, 2938, 2850, 2797, 2744, 1651, 1590, 1490, 1471, 1453, 1394, 1348, 1329, 1287, 1254, 1187, 1167, 1133, 1090, 1066, 1039, 1006, 942, 816, 789, 736, 673, 657, 629, 585, 545, 506, 434, 406 cm^{-1}. **HRMS (ESI):** calculated mass for $C_{16}H_{25}N_2O_3S$ $[M+H]^+$: 325.1586; found: 325.1578. **EA:** analysis calculated for $C_{16}H_{24}N_2O_3S$: C 59.23, H 7.46, N 8.63; found: C 59.13, H 8.44, N 8.60

Complex Sil-II:
Dry Schlenk vessel was charged with ruthenium complex **Ind-II** (100 mg, 0.105 mmol, 1 equiv.) under argon atmosphere. Then, 15 mL of anhydrous toluene was added, resulting in a deep red solution. Styrene **2** (34 mg, 0.105 mmol, 1 equiv.) and $CuCl_{anh}$ (15 mg, 0.158 mmol, 1.5 equiv.) were added to this solution. Reaction mixture was stirred and heated up to 60 °C. After 30 minutes, TLC (stationary phase: SiO_2, eluent: EtOAc/*n*-hexane 10:90 v/v, $R_{F,\mathbf{Ind\text{-}II}}$ = 0.39, $R_{F,Sil\text{-}II'}$ = 0) was performed in order to control the progress of the reaction. No spot from **Ind-II** could be observed. All the volatiles were removed under reduced pressure and the crude product was purified using column chromatography (stationary phase: SiO_2, eluent: EtOAc/*n*-hexane from 0:100 to 50:50 v/v). Product **Sil-II** was obtained as a green solid (67 mg, 82%). **^{1}H NMR (400 MHz, CD_2Cl_2) δ:** 16.31 (s, 1H), 7.94 (dd, *J* = 8.7, *J* = 2.1 Hz, 1H), 7.30 (d, *J* = 2.1 Hz, 1H), 7.10 (s, 4H), 7.00 (d, *J* = 8.6 Hz, 1H), 4.25 (q, *J* = 7.0 Hz, 2H), 4.20 (s, 4H), 3.02 (bs, 4H), 2.41-2.47 (m, 22 H), 2.25 (s, 4H), 1.17 (t, *J* = 7.0 Hz, 3H). **^{13}C NMR (101 MHz, CD_2Cl_2) δ:** 290.0, 208.9, 156.6, 144.5, 139.5, 139.4, 131.4, 129.7, 128.8, 121.1, 112.8, 68.2, 54.5, 51.9, 46.2, 45.9, 32.3, 29.41, 23.1, 21.2, 19.5, 14.3, 13.7. **FT-IR (CH_2Cl_2 film):** 2918, 2853, 2798, 2743, 1730, 1605, 1577, 1483, 1453, 1423, 1399, 1350, 1317, 1264, 1164, 1149, 1135, 1111, 1092, 1022, 946, 900, 853, 811, 788, 735, 673, 646, 625, 611, 568, 504, 424 cm^{-1}. **HRMS (ESI):** calculated mass for $C_{35}H_{46}N_4O_3SClRu$ $[M-Cl]^+$: 739.2023; found: 739.2002.

Complex Sil-II':
In a Schlenk flask, to a suspension of NHC precursor **SIPr•HCl** (156 mg, 0.365 mmol, 1.20 equiv.) in dry toluene (10 mL), LiHMDS (0.35 M in toluene, 891 mg, 1 mL, 0.350 mmol, 1.15 equiv.) solution was added dropwise at 20 °C and the resulting mixture was stirred for 20 minutes until the suspension became almost completely clear (homogenous). The resulting mixture was transferred to a Schlenk flask containing the solution of **Ind-I** (281 mg, 0.304 mmol, 1 equiv.)/**Gru-I** (250 mg, 0.304 mmol, 1 equiv.) in dry toluene (10 mL) and was stirred at 70 °C for 2 hours. The progress of the reaction was monitored by TLC (stationary phase: SiO_2, eluent: EtOAc/*n*-hexane 5:95 v/v). Then, styrene **2** (99 mg, 0.304 mmol, 1 equiv.) and $CuCl_{anh}$ (67 mg, 0.670 mmol, 2.2 equiv) were added and the resulting mixture was stirred at 80 °C for 1 hour. The progress of the reaction was monitored by TLC (stationary phase: SiO_2, eluent: EtOAc/*n*-hexane – 50:50 v:v). When the reaction reached completion, the volatiles were removed under the reduced pressure (up to the volume ~3 mL) and the crude was purified using column chromatography (stationary phase: SiO2, eluent: EtOAc/*n*-hexane from 50:50 to 100:0 v/v). The product was obtained as green solid (starting from **Ind-I**: 123 mg, 43%; starting from **Gru-I**: 176 mg, 61%), which turned out to be an ethyl acetate solvate. **^{1}H NMR (400 MHz, CD_2Cl_2) δ:** 16.24 (d, *J* = 0.7 Hz, 1H), 7.87 (dd, *J* = 8.6, 2.2 Hz, 1H), 7.58 – 7.54 (m, 2H), 7.38 (d, *J* = 7.8 Hz, 4H), 7.17 (d, *J* = 2.2 Hz, 1H), 7.01 (d, *J* = 8.3 Hz, 1H), 4.31 (q, *J* = 7.0 Hz, 2H), 4.19 (s, 4H), 3.54 (hept, *J* = 6.7 Hz, 4H), 2.93 (s, 4H), 2.42 (s, 4H), 2.22 (s, 3H), 1.35 (t, *J* = 7.0 Hz, 3H), 1.26 (d, *J* = 6.8 Hz, 12H), 1.20 (d, *J* = 6.6 Hz, 12H). **^{13}C NMR (101 MHz, CD_2Cl_2) δ:** 284.5, 212.7, 158.3, 151.0, 145.0, 138.5, 132.4, 131.6, 130.1, 126.3, 122.3, 114.3, 69.9, 62.1, 56.5, 47.7, 30.6, 28.1, 27.8, 25.1, 16.2, 15.9, 2.7. **FT-IR (CH_2Cl_2 film):** 3063, 2966, 2929, 2867, 2800, 1736, 1683, 1577, 1458, 1411, 1391, 1352, 1328, 1265, 1236, 1165, 1148, 1091, 1063, 1024, 946, 901, 806, 760, 735, 703, 646, 625, 566, 504, 457 cm^{-1}. **HRMS (ESI):** calculated mass for $C_{41}H_{59}Cl_2N_4O_3RuS$ $[M+H]^+$: 859.2728; found: 859.2722. **EA:** analysis calculated for $C_{45}H_{66}Cl_2N_4O_5RuS$ (**Sil-II'** + EtOAc): C 57.07, H 7.02, Cl 7.49, N 5.92, O 8.45, Ru 10.67, S 3.39; found: C 57.21, H 7.05, Cl 7.48, N 6.10, S 3.35. **UV-Vis:** λ_{max} = 367 nm.

General procedure for RCM catalyzed by Sil-II':
Under argon atmosphere, the substrate **3a-3h** (118-274 mg, 0.5/1.0 mmol, 1 equiv.) was placed in the Schlenk flask. Then, 4.5-9.0 mL of dry DCM from ampula was added. Stock solution of the catalyst **Sil-II'** (4.8 mg, 0.005 mmol, 1 M) in DCM (5 mL) was prepared. 0.5/1.0 mL of the resulting stock solution was added to the reaction mixture (0.48/0.96 mg, 0.0005/0.0010 mmol, 0.1 mol%). The concentration of the solution obtained is 0.1 M. It was stirred at room temperature for 1-2 hours until the completion of the RCM reaction was reached (progress of the reaction was monitored using TLC). Then, SnatchCat solution (4.4 equiv. vs the catalyst, 0.44 mol%) was added in order to quench the reaction progress. The products **4a-4h** were purified using column chromatography (stationary phase: SiO_2, eluent: EtOAc/*n*-hexane).

General procedure for CM catalyzed by Sil-II':
Alkene (1 equiv.) and the cross partner (2-3 equiv.) were dissolved in dry DCM under argon atmosphere. To the resulting mixture, the solution of the catalyst **Sil-II'** (0.2-0.5 mol%) was added and the mixture was stirred at rt. After reaction completion, it was quenched using ethyl vinyl ether or SnatchCat (4.4 equiv. vs the catalyst). All the volatiles were removed under reduced pressure and the crude product was purified using column chromatography (stationary phase: SiO_2, eluent: EtOAc/*n*-hexane).

CCDC 2086445, 2086446 and 2086447 contain the supplementary crystallographic data for this paper. These data can

be obtained freely via http://www.ccdc.cam.ac.uk/data_request/cif, by e-mailing data_request@ccdc.cam.ac.uk or by contacting directly the Cambridge Crystallographic Data Centre (12 Union Road, Cambridge CB2 1EZ, UK. Fax: +44 1223 336033).

Acknowledgements

Authors are grateful to the „Catalysis for the Twenty-First Century Chemical Industry" project carried out within the TEAM-TECH programme of the Foundation for Polish Science co-financed by the European Union from the European Regional Development under the Operational Programme Smart Growth. The study was carried out at the Biological and Chemical Research Centre, University of Warsaw, established within the project co-financed by European Union from the European Regional Development Fund under the Operational Programme Innovative Economy, 2007–2013. Authors are grateful to Dr. Michał Chmielewski for granting access to his equipment and to Dr. Jakub Karasiński for the help.

References

1. (a) G. Brahmachari, *RSC Adv.* **2016,** *6*, 64676-64725; (b) V. Nair, S. Vellalath, B. P. Babu, *Chem. Soc. Rev.* **2008,** *37*, 2691-2698.
2. E. J. Corey, C. Xue-Min, *The Logic of Chemical Synthesis*. John Wiley & Sons: Chichester, 1989.
3. (a) A. H. Hoveyda, A. R. Zhugralin, *Nature* **2007,** *450*, 243-251; (b) *Handbook of Metathesis*, R. H. Grubbs, A. G. Wenzel, D. J. O'Leary, E. Khosravi, Eds. Wiley-VCH: Weinheim, **2015**. (c) *Olefin Metathesis: Theory and Practice*. (Ed. K. Grela) Wiley: Hoboken, **2014**.
4. *Metathesis in Natural Product Synthesis: Strategies, Substrates and Catalysts*. (Ed. J. Cossy, S. Arseniyadis, C. Meyer) Wiley-VCH: Weinheim, **2010**.
5. (a) T. M. Trnka, R. H. Grubbs, *Acc. Chem. Res.* **2001,** *34*, 18-29; (b) P. Schwab, R. H. Grubbs, J. W. Ziller, *J. Am. Chem. Soc.* **1996,** *118*, 100-110.
6. O. M. Ogba, N. C. Warner, D. J. O'Leary, R. H. Grubbs, *Chem. Soc. Rev.* **2018,** *47*, 4510-4544.
7. M. Scholl, S. Ding, C. W. Lee, R. H. Grubbs, *Org. Lett.* **1999,** *1*, 953-956.
8. (a) A. Fürstner, J. Grabowski, C. W. Lehmann, *J. Org. Chem.* **1999,** *64*, 8275-8280; (b) L. Jafarpour, H.-J. Schanz, E. D. Stevens, S. P. Nolan, *Organometallics* **1999,** *18*, 5416-5419; (c) A. Fürstner, O. Guth, A. Düffels, G. Seidel, M. Liebl, B. Gabor, R. Mynott, *Chem. Eur. J.* **2001,** *7*, 4811-4820; (d) F. Boeda, H. Clavier, S. P. Nolan, *Chem. Commun.* **2008**, 2726-2740.
9. S. B. Garber, J. S. Kingsbury, B. L. Gray, A. H. Hoveyda, *J. Am. Chem. Soc.* **2000,** *122*, 8168-8179.
10. (a) M. Mauduit, T. Schmid, A. Dumas, S. Colombel-Rouen, C. Crévisy, O. Baslé, *Synlett* **2017,** *28*, 773-798; (b) T. K. Olszewski, M. Bieniek, K. Skowerski, K. Grela, *Synlett* **2013,** *24*, 903-919.
11. (a) K. Grela, S. Harutyunyan, A. Michrowska, *Angew. Chem., Int. Ed.* **2002,** *41*, 4038-4040; (b) A. Michrowska, R. Bujok, S. Harutyunyan, V. Sashuk, G. Dolgonos, K. Grela, *J. Am. Chem. Soc.* **2004,** *126*, 9318-9325.
12. Z.-Y. Zhan, **2007** Ruthenium complex ligand, ruthenium complex, carried ruthenium complex catalyst and the preparing methods and the use thereof. WO2007003135A1.
13. H. Clavier, F. Caijo, E. Borré, D. Rix, F. Boeda, S. P. Nolan, M. Mauduit, *Eur. J. Org. Chem.* **2009,** *2009*, 4254-4265.
14. A. Kajetanowicz, K. Grela, *Angew. Chem., Int. Ed.*, DOI: 10.1002/anie.202008150
15. For a discussion on various synthetic strategies in preparation of substituted chelating benzylidene ligands precursors see: R. Bujok, M. Bieniek, M. Masnyk, A. Michrowska, A. Sarosiek, H. Stępowska, D. Arlt, K. Grela, *J. Org. Chem.* **2004,** *69*, 6894-6896.
16. A. Michrowska, K. Grela, *Pure Appl. Chem.* **2008,** *80*, 31-43.
17. Eur-Lex (European Union Law) - A new Circular Economy Action Plan for a Cleaner and More Competitive Europe, 2020 https://eur-lex.europa.eu/resource.html?uri=cellar:9903b325-6388-11ea-b735-01aa75ed71a1.0017.02/DOC_1&format=PDF (accessed on July 19, 2021)
18. H. C. Erythropel, J. B. Zimmerman, T. M. de Winter, L. Petitjean, F. Melnikov, C. H. Lam, A. W. Lounsbury, K. E. Mellor, N. Z. Janković, Q. Tu, L. N. Pincus, M. M. Falinski, W. Shi, P. Coish, D. L. Plata, P. T. Anastas, *Green Chem.* **2018,** *20*, 1929-1961.
19. (a) P. J. Dunn, *Org. Process Res. Dev.* **2005,** *9*, 88-97; (b) M. A. Gouda, W. S. Hamama, *Synth. Commun.* **2017,** *47*, 1269-1300; (c) M. Vardi, A. Nini, *Cochrane Database Syst. Rev.* **2007**,
20. R.-C. Wang, F.-M. Jiang, Q.-L. Zheng, C.-T. Li, X.-Y. Peng, C.-Y. He, J. Luo, Z.-A. Liang, *Respir. Med.* **2014,** *108*, 531-537.
21. Pfizer 2019 Financial Record: https://s21.q4cdn.com/317678438/files/doc_financials/2018/ar/Pfizer-2019-Financial-Report.pdf (accessed on July 19, 2021)
22. "The Top 300 of 2021". ClinCalc. https://clincalc.com/DrugStats/Top300Drugs.aspx (accessed on July 19, 2021)
23. For Hoveyda-Grubbs type catalysts with modified etheral parts, see: (a) M. Barbasiewicz, M. Bieniek, A. Michrowska, A. Szadkowska, A. Makal, K. Woźniak, K. Grela, *Adv. Synth. Catal.* **2007,** *349*, 193-203; (b) P. Kos, R. Savka, H. Plenio, *Adv. Synth. Catal.* **2013,** *355*, 439-447; (c) K. M. Engle, G. Lu, S.-X. Luo, L. M. Henling, M. K. Takase, P. Liu, K. N. Houk, R. H. Grubbs, *J. Am. Chem. Soc.* **2015**, *137*, 5782-5792; (d) K. M. Engle, S.-X. Luo, R. H. Grubbs, *J. Org. Chem.* **2015**, *80*, 4213-4220; (e) A. Zieliński, G. Szczepaniak, R. Gajda, K. Woźniak, B. Trzaskowski, D. Vidović, A. Kajetanowicz, K. Grela, *.Eur. J. Inorg. Chem.* **2018**, *2018*, 3675-3685.
24. (a) S. Monsaert, R. Drozdzak, V. Dragutan, I. Dragutan, F. Verpoort, *Eur. J. Inorg. Chem.* **2008**, *2008*, 432-440; (b) R. Dorta, R. A. Kelly III, S. P. Nolan, *Adv. Synth. Catal.* **2004**, *346*, 917-920.
25. M. Barbasiewicz, A. Szadkowska, A. Makal, K. Jarzembska, K. Woźniak, K. Grela, *Chem. Eur. J.* **2008**, *14*, 9330-9337.
26. (a) E. Despagnet-Ayoub, R. H. Grubbs, *Organometallics* **2005**, *24*, 338-340; (b) M. Pieczykolan, J. Czaban-Jozwiak, M. Malinska, K. Wozniak, R. Dorta, A. Rybicka, A. Kajetanowicz, K. Grela, *Molecules* **2020**, *25*,
27. A. Addison, T. N. Rao, J. Reedijk, J. van Rijn, G. C. Verschoor, *J. Chem. Soc., Dalton Trans.* **1984**, 1349-1356.
28. T. Ritter, A. Hejl, A. G. Wenzel, T. W. Funk, R. H. Grubbs, *Organometallics* **2006**, *25*, 5740-5745.
29. The relative initiation rate value was obtained from the ratio of the observed initiation rate k_{init} of the reaction catalyzed by the different complexes and the k_{init} of reaction with **Sil-II'**. k_{rel}(**X**) = k_{init}(**X**)/k_{init}(**Sil-II'**) and k_{init} was obtained from v=k_{init}[**3a**] where **X** is **Gre-II'**, **Gre-II**, **Hov-II'**, **Hov-II**, **Mau-II'**, **Zha-II** or **Sil-II**.
30. C. Hansch, A. Leo, R. W. Taft, *Chem. Rev.* **1991**, *91*, 165-195.
31. M. Zaja, S. J. Connon, A. M. Dunne, M. Rivard, N. Buschmann, J. Jiricek, S. Blechert, *Tetrahedron* **2003**, *59*, 6545-6558.
32. The Hammett parameters is assumed to be very similar than the one of SO_2NMe_2 since the functional group are very similar. Moreover, SO_2NH_2, SO_2NHPh and SO_2NMe_2 got some very

similar Hammett parameters values (0.60; 0.53, 0.65; 0.56 and 0.65; 0.51 respectively) which tend to confirm the validity of this approximation.
33. V. Thiel, M. Hendann, K.-J. Wannowius, H. Plenio, *J. Am. Chem. Soc.* **2012**, *134*, 1104-1114.
34. S. H. Hong, D. P. Sanders, C. W. Lee, R. H. Grubbs, *J. Am. Chem. Soc.* **2005**, *127*, 17160-17161.
35. S. J. Connon, S. Blechert, *Angew. Chem., Int. Ed.* **2003**, *42*, 1900-1923.
36. Ł. Woźniak, A. A. Rajkiewicz, L. Monsigny, A. Kajetanowicz, K. Grela, *Org. Lett.* **2020**, *22*, 4970-4973.
37. A. K. Chatterjee, T.-L. Choi, D. P. Sanders, R. H. Grubbs, *J. Am. Chem. Soc.* **2003**, *125*, 11360-11370.
38. G. A. Bailey, D. E. Fogg, *J. Am. Chem. Soc.* **2015**, *137*, 7318-7321.
39. J. Fischer, C. R. Ganellin, *Analogue- based Drug Discovery*. (Ed. IUPAC, J. Fischer, C. R. Ganellin) John Wiley & Sons: **2006**.
40. G.-W. Chen, A. Kirschning, *Chem. Eur. J.* **2002**, *8*, 2717-2729.
41. A. D. William, A. C. H. Lee, S. Blanchard, A. Poulsen, E. L. Teo, H. Nagaraj, E. Tan, D. Chen, M. Williams, E. T. Sun, K. C. Goh, W. C. Ong, S. K. Goh, S. Hart, R. Jayaraman, M. K. Pasha, K. Ethirajulu, J. M. Wood, B. W. Dymock, *J. Med. Chem.* **2011**, *54*, 4638-4658.
42. X. Shen, T. T. Nguyen, M. J. Koh, D. Xu, A. W. H. Speed, R. R. Schrock, A. H. Hoveyda, *Nature* **2017**, *541*, 380-385.
43. (a) M. A. Gouda, *Synth. Commun.* **2017**, *47*, 2269-2304; (b) K. Hatzimouratidis, *Ther. Adv. Urol.* **2014**, *6*, 135-147.
44. L. Piola, F. Nahra, S. P. Nolan, *Beilstein J. Org. Chem.* **2015**, *11*, 2038-2056.
45. G. Szczepaniak, S. J. Czarnowski, K. Skowerski. Use of Metal Scavengers for Removal of Ruthenium Residues. WO/2014/174501, **2014**; (b) G. Szczepaniak, J. Piątkowski, W. Nogaś, F. Lorandi, S. S. Yerneni, M. Fantin, A. Ruszczyńska, A. E. Enciso, E. Bulska, K. Grela, K. Matyjaszewski, *Chem. Sci.* **2020**, *11*, 4251-4262; (c) G. Szczepaniak, K. Urbaniak, C. Wierzbicka, K. Kosiński, K. Skowerski, K. Grela, *ChemSusChem* **2015**, *8*, 4139-4148.
46. A. Michrowska, Ł. Gułajski, K. Grela, *Chem. Commun.* **2006**, 841-843.
47. J. Sherwood, *Angew. Chem., Int. Ed.* **2018,** *57*, 14286-14290.
48. D. Prat, A. Wells, J. Hayler, H. Sneddon, C. R. McElroy, S. Abou-Shehada, P. J. Dunn, *Green Chem.* **2016,** *18*, 288-296.
49. **3a** was chosen as standard substrate for this study since Plenio and co-workers demonstrated that it was a limit case for which only one activation mechanism (*e.g.* dissociative or interchange mechanism, depicted in Figure 8) was involved mainly because of the steric and electronic properties of **3a**.
50. T. Vorfalt, K.-J. Wannowius, H. Plenio, *Angew. Chem., Int. Ed.* **2010,** *49*, 5533-5536.
51. R. Poli, *Comments Inorg. Chem.* **2009,** *30*, 177-228.

10.1002/adsc.202100669

RESEARCH ARTICLE

Activated Hoveyda-Grubbs Olefin Metathesis Catalysts Derived from a Large Scale Produced Pharmaceutical Intermediate—Sildenafil Aldehyde

Adv. Synth. Catal. **Year**, *Volume*, Page – Page

L. Monsigny, J. Piątkowski, D. Trzybiński, K. Woźniak, T. Nienałtowski, A. Kajetanowicz,* K. Grela*